

Photoinduced Rydberg Ionization Spectroscopy of Phenylacetylene: Vibrational Assignments of the \tilde{C} State of the Cation

Haifeng Xu and Philip M. Johnson*

Chemistry Department, Stony Brook University, Stony Brook, New York 11974

Trevor J. Sears

Department of Chemistry, Brookhaven National Laboratory, Upton, New York 11973-5000

Received: March 9, 2006; In Final Form: May 1, 2006

The photoinduced Rydberg ionization spectrum of the third excited electronic state of phenylacetylene cation was recorded via the origin of the cation ground electronic state. The origin of this state is $17\,834\text{ cm}^{-1}$ above the ground state of the cation, and the spectrum shows well-resolved vibrational features to the energy of 2200 cm^{-1} above this. An assignment of the vibrational structure was made by comparison to calculated frequencies and Franck–Condon factors. From the assignments, and electronic structure considerations, the electronic symmetry of the \tilde{C} state is established to be ${}^2\text{B}_1$.

Introduction

In all substituted benzene cations, the \tilde{B} and \tilde{C} states lie very close to one another, and the ordering of the symmetries varies with the substituent. These two states are formed from the removal of an electron from either the highest $2p\ \sigma$ orbital or from one of the two orbitals formed from the interaction of the lowest ring π orbital with a $2p$ or π orbital on the substituent.¹ The former symmetry (in C_{2v}) is ${}^2\text{B}_2$, and the latter is ${}^2\text{B}_1$. In benzene and phenol, the energy of the ${}^2\text{B}_2\ \sigma$ state is below that of ${}^2\text{B}_1$, whereas in fluorobenzene and chlorobenzene that ordering is reversed because of the interaction of the halogen out-of-plane $2p$ orbital with the ring.¹ In phenylacetylene, there is a more extensive π system on the acetylene group, and it is of interest to confirm the σ – π ordering in this molecule.

Because the cation ground state is ${}^2\text{B}_1$, transitions from there to ${}^2\text{B}_1$ and ${}^2\text{B}_2$ states are quite distinct because the former is electronically allowed and the latter forbidden. An accurate vibrational analysis therefore easily allows an electronic assignment.

In the past fifteen years or so, high-resolution studies of polyatomic cations have blossomed with the advent of zero kinetic energy (ZEKE) spectroscopy² and mass analyzed threshold ionization (MATI) spectroscopy.³ These techniques have, with the exception of few cases, been applied to study the ground electronic state of the cations. Photoelectron spectroscopy (PES) is regarded as a useful spectroscopic technique to study the excited electronic states of polyatomic cations.⁴ However, the resolution of PES is typically 10 meV at best, which is not sufficient to get spectra with vibrational or rotational resolution for most, larger polyatomic cations.

Photoinduced Rydberg ionization (PIRI) spectroscopy, which was first introduced by our laboratory,^{5,6} has proven to be well suited for vibrational resolved studies of excited states of molecular ions. This technique relies upon the fact that the high- n Rydberg electrons interact very little with optical radiation or core orbitals. Therefore, the absorption cross section of a Rydberg molecule, in the visible or UV region, is almost exactly the same as the corresponding bare ion. As in MATI,

the directly produced ions are spatially separated from the neutral Rydberg molecules using small electric fields. However, instead of using field ionization to detect the formation of Rydbergs, a tunable laser beam (PIRI laser) is employed to induce ionization by optically exciting the ion core of the Rydberg molecules. The high-resolution spectra of the excited electronic states of the cations are then obtained by scanning the PIRI laser. When core absorption occurs, a signal is seen due to rapid autoionization to parent ions (parent PIRI) or fragment ions generated by absorption of further photons to a dissociation state (fragment PIRI).⁶ Since it was developed, PIRI spectroscopy has been successfully applied to study the \tilde{B} states of benzene and perdeuteriobenzene cations,⁷ as well as the substituted benzene cations, phenol and phenol- d_6 ,⁸ fluorobenzene,⁹ and chlorobenzene.¹⁰

Phenylacetylene provides a contrast to these because of its π -bonded substituent. The spectroscopy and structure of the excited and ground electronic states of neutral phenylacetylene have been well studied using various experimental techniques,^{11–13} supported by ab initio calculations.^{14,15} PES,^{16,17} threshold photoelectron spectroscopy (TPES)¹⁸ and recently one-photon MATI spectroscopy¹⁹ studies have also been carried out. The lowest ionization potential (IP = 8.8195 eV) and the vibrational frequencies of the ground ionic state were established by the MATI spectrum.¹⁹ PES studies^{16,17} have determined the IP of the excited \tilde{B} and \tilde{C} state to be 10.33 and 11.03 eV, respectively. That work assigned a B_1 symmetry to the \tilde{C} state by reference to electronic structure calculations. However, a detailed study of the spectrum of the \tilde{C} state of phenylacetylene cation, as would be required for an unambiguous experimental assignment, has not been previously reported.

Experiment

The apparatus used here to obtain PIRI spectrum of phenylacetylene cation is similar to that used for the PIRI studies of benzene and substituted benzenes, and has been described in detail previously.^{7–9} Briefly, jet cooled phenylacetylene molecules were excited to the high- n Rydberg states by a resonant

two-color two-photon process. A third tunable dye laser was used as the PIRI laser, and the vibrational spectrum of the \tilde{C} ionic state was obtained by detecting parent PIRI ions while scanning the PIRI laser.

Phenylacetylene was purchased from Aldrich and used without any purification. A jet-cooled molecular beam was produced from a supersonic expansion of phenylacetylene (seeded with He gas in room temperature with backing pressure of ~ 2.7 atm) through a pulsed nozzle (300 μ m orifice diameter) and was introduced to the ionization chamber through a skimmer (3 mm diameter) placed about 4 cm downstream from the nozzle. Typical pressure in the source chamber was in the 1×10^{-5} Torr range, and that in the ionization region was between 7×10^{-7} and 2×10^{-6} Torr.

Three laser systems were used in the experiment to record the PIRI spectrum. Rydberg-excited phenylacetylene was created by resonant enhanced (1+1') process using two different dye laser systems, both of which were frequency doubled to produce the ultraviolet outputs. To reduce the rotational state congestion in the ion, a very high-resolution (~ 100 MHz) laser system, an Ar⁺ pumped cw ring dye laser (Coherent 699-29) which is pulse amplified by a seeded Nd:YAG laser (Quanta Ray GCR200), was used as the first laser to excite the neutral phenylacetylene to a single rotational state of its S₁ excited electronic state. The second laser system, a Quanta-Ray PDL1 dye laser (line width ~ 0.2 cm⁻¹) pumped by a Nd:YAG laser (Quantel), was then used to create Rydbergs converging to the origin of the ground ionic state. The two laser beams, which were counter-propagating and both perpendicular to the molecular beam, were spatially overlapped in the molecule-laser interaction region with a time delay of about 30 ns between the pulses. The typical ultraviolet output power of the pulse amplified continuous wave (cw) laser was about 0.5 mJ/pulse, and that of the second dye laser was about 1 mJ/pulse. The visible output of the third dye laser (the PIRI laser), which is a Lumonics HD300 dye laser (line width ~ 0.2 cm⁻¹) pumped by another Quantel Nd:YAG laser, was introduced down the molecule beam at a time delay, which is typically 3 μ s after the formation of intermediate Rydbergs. By scanning the wavelength of the PIRI laser, one can obtain the vibrational structure of the $\tilde{C}-\tilde{X}$ transition of the cation. Various dyes were used in the PIRI laser to cover the scanning wavelength range between 500 and 570 nm. The wavelengths were calibrated using a wavemeter. The power of the visible output of the PIRI laser was typically about 6 mJ/pulse. To avoid power broadening, none of the lasers were focused.

The voltage separation scheme used in the PIRI technique to separate and detect the three packets of ions in the ionization region has been described in detail previously in ref 6. As discussed there, there are two different setups in PIRI technique, namely parent PIRI and fragment PIRI. For phenylacetylene cation, it is possible to use either technique to record the spectrum, as opposed to the phenol case⁸ where only fragment PIRI could be used. In the present study, the parent detection was chosen, because the line widths of vibrational transitions are usually substantially broadened in fragment PIRI because those spectra are actually resonances in a multiphoton excitation to a high-energy dissociating state.⁶

Because of the small number of Rydberg molecules comprising the initial state of a PIRI transition, the dynamic range for the signal is not very large. This is particularly true for parent PIRI, where there is an inherent background signal caused by separation voltage switching,⁶ so there is only a small range from when a signal rises above the background to its being saturated by depletion of the initial state. Often when weak lines

in the spectrum are visible at all, the strong lines tend to be saturated, and intensities in the spectrum are not representative of the oscillator strengths. For comparison between a simulated spectrum and an experimental one, it is often useful to plot the square root of the intensity in the simulation. That is what has been done here.

Calculations

Because the primary candidate for the symmetry of the \tilde{C} state is 2B_1 ,^{16,17} the same as the ground state, non-CI methods are not an option for electronic structure calculations. The geometry, energy, and vibrations were therefore determined using the MCSCF method of the Gamess program.²⁰ The active space was composed of the eight orbitals of π character, and a 6-31G (2d,p) basis set was used. A similar calculation was done on the cation ground state, yielding an excitation energy of 2.425 eV (versus 2.211 eV experimentally for the 0–0 transition). This is a 1726 cm⁻¹ discrepancy, of which 177 cm⁻¹ is attributable to the zero-point correction. The geometries of the two states are quite similar, with the bond lengths of the \tilde{C} state being slightly longer, in general.

Franck–Condon (FC) factors were calculated from the MCSCF vibrational vectors using the program MolFC, written and distributed by R. Borrelli and A. Peluso.²¹ These FC factors include all effects of geometry change between the states, and Duschinsky rotation. Vibrational frequencies and $\tilde{C}-\tilde{X}$ FC factors for the fundamental vibrations are presented in Table 1.

Results and Discussion

The parent PIRI spectrum of the \tilde{C} state via the origin of the ground ionic state (\tilde{X}^2B_1) is shown in Figure 1. The origin of the \tilde{C} state, which corresponds to the most intense peak in the spectrum, is at the energy of 17 834 cm⁻¹ above the ground ionic state, corresponding to approximately the same value of 11.03 eV (from the neutral ground state) obtained in the PES studies by Rabalias et al.¹⁶ and Lichtenberger et al.¹⁷ Well-resolved vibrational peaks were observed in the entire studied energy range of 0–2200 cm⁻¹ above the \tilde{C} state origin. One main vibrational progression was found, along with dense structure at higher energy. The progressions are not as extensive and anharmonic as were observed in the PIRI spectra of phenol cation obtained in our laboratory previously,⁷ indicating no major geometry change on excitation. The widths of the vibrational peaks, which are approximately in the range of 20–40 cm⁻¹, are much larger than those in the PIRI spectra of the \tilde{B} states of other substitute benzenes, which are typically smaller than 10 cm⁻¹.^{8–10} One possible reason for the line broadening is that the \tilde{C} state predissociates, an argument supported by the fact that fragment ions can be observed during the experiment even without focusing the PIRI laser. Another possibility is that the vibrational levels of the \tilde{C} state may be interacting with the higher vibrational levels of the nearby \tilde{B} state. Of course, both predissociation and state interaction may be occurring simultaneously.

The phenylacetylene cation, with C_{2v} symmetry, has 36 nondegenerate normal modes, 13 of which belong to a₁ symmetry, 3 to a₂, 8 to b₁ and 12 to b₂. Assigning its vibrational spectrum can be difficult for a molecule that has such a large number of vibrational degrees of freedom, especially when no additional information is available. To make a reliable assignment of the spectrum, the frequencies and FC factors listed in Table 1 were used. The vibrational frequencies of the ground ionic state obtained by Kim et al.¹⁹ are also listed in the table. Both Wilson's²² and Herzberg's²³ notations for the vibrational

TABLE 1: Calculated and Experimental Vibrational Frequencies (in cm^{-1}) of the Phenylacetylene Cation in the Ground State^a and \tilde{C}^2B_1 Excited State^b

| vibrational modes | | | ground state ^a | | \tilde{C}^2B_1 state ^b | |
|-------------------|----------|----------|---------------------------|------|-------------------------------------|------|
| Wilson | Herzberg | symmetry | BP86 | MATI | calc | PIRI |
| 1 | 12 | a_1 | 746 | 747 | 728 | |
| 2 | 2 | a_1 | 3144 | | 3123 | |
| 3 | 30 | b_2 | 1257 | 1287 | 1317 | |
| 4 | 20 | b_1 | 699 | 706 | 622 | |
| 5 | 17 | b_1 | 999 | 996 | 933 | |
| 6a | 13 | a_1 | 455 | 458 | 447 | 448 |
| 6b | 34 | b_2 | 560 | 561 | 612 | 539 |
| 7a | 4 | a_1 | 3119 | | 3103 | |
| 7b | 25 | b_2 | 3142 | | 3118 | |
| 8a | 6 | a_1 | 1592 | 1604 | 1552 | 1548 |
| 8b | 27 | b_2 | 1483 | 1505 | 1594 | |
| 9a | 9 | a_1 | 1172 | 1185 | 1137 | 1116 |
| 9b | 31 | b_2 | 1139 | 1158 | 1158 | |
| 10a | 15 | a_2 | 789 | 795 | 796 | |
| 10b | 24 | b_1 | 115 | 110 | 130 | 126 |
| 11 | 19 | b_1 | 787 | 795 | 724 | |
| 12 | 11 | a_1 | 971 | 979 | 912 | 939 |
| 13 | 8 | a_1 | 1228 | 1249 | 1164 | 1147 |
| 14 | 29 | b_2 | 1348 | | 1351 | |
| 15 | 36 | b_2 | 145 | 143 | 159 | 148 |
| 16a | 16 | a_2 | 345 | 346 | 368 | |
| 16b | 22 | b_1 | 457 | | 372 | 368 |
| 17a | 14 | a_2 | 982 | 989 | 919 | |
| 17b | 18 | b_1 | 949 | | 842 | 843 |
| 18a | 10 | a_1 | 981 | | 990 | 996 |
| 18b | 32 | b_2 | 1081 | 1076 | 1071 | |
| 19a | 7 | a_1 | 1435 | 1435 | 1478 | 1467 |
| 19b | 28 | b_2 | 1399 | | 1457 | |
| 20a | 3 | a_1 | 3133 | | 3113 | |
| 20b | 26 | b_2 | 3130 | | 3106 | |
| βCC | 35 | b_2 | 507 | 499 | 521 | |
| βCH | 33 | b_2 | 645 | 658 | 749 | |
| νCC | 5 | a_1 | 2053 | 2040 | 2005 | |
| νCH | 1 | a_1 | 3334 | | 3235 | |
| γCC | 23 | b_1 | 311 | 303 | 335 | 335 |
| γCH | 21 | b_1 | 621 | 622 | 479 | 479 |

^a From ref 19. ^b This work.

modes are shown in the table. For the discussions of the assignment, we prefer Wilson's notation, so comparison can be made with benzene and other substitute benzenes. On the basis of the calculated frequencies, Franck–Condon factors, as well as symmetry analysis, a nearly complete assignment has been made for the spectrum shown in Figure 1.

As indicated in the literature,^{17,18} both the \tilde{X} and the \tilde{C} states of phenylacetylene cation have B_1 symmetry, an assignment also supported by our calculations and the fact that no weaker lines appear to the red of the first intense peak. If the state had B_2 symmetry, one would expect a strong false origin on an a_2 vibration (because of vibronic coupling to a nearby B_1 state) and weaker, lower energy false origins on b_1 and/or b_2 vibrations. Searches for such low-energy weak lines failed, even using very high laser powers.

Because the PIRI spectrum was recorded from the vibrationless level of the ground state, transitions to upper vibrational states with a_1 symmetry should have the most intensity. In the 0–2200 cm^{-1} vibrational energy range, there are 9 a_1 vibrational modes, namely, 1, 6a, 8a, 9a, 12, 13, 18a, 19a, and ν_{CC} (the acetylene CC stretch). The calculated Franck–Condon factors for the fundamentals 6a, 9a and 19a are especially significant, with calculated frequencies at 447, 1137 and 1478 cm^{-1} , respectively. Thus, the prominent peaks at 448, 1116 and 1467 cm^{-1} in the PIRI spectrum can be readily assigned as 6a¹, 9a¹ and 19a¹, respectively. The fundamentals of the other four a_1 modes, 12¹, 18a¹, 13¹ and 8a¹, have rather smaller calculated

TABLE 2: Assignment of the PIRI Spectrum of Phenylacetylene Cation in the \tilde{C}^2B_1 Excited State

| vibrational modes ^{a,b} | frequency (cm^{-1}) | | | intensity ^d | |
|------------------------------------------------------|--------------------------------|------|------------------------------------|------------------------|------|
| | exp | calc | $\delta(\text{exp} - \text{calc})$ | calc | exp |
| 10b ² | 251 | 259 | −8 | 0.002 | 0.25 |
| 15 ² | 296 | 318 | −22 | 0.0002 | 0.14 |
| 6a ¹ | 448 | 447 | +1 | 0.7 | 0.50 |
| 6b ¹ | 539 ^c | 612 | −73 | 0 | 0.13 |
| 10b ¹ 16b ¹ | | 503 | +36 | 0.0005 | |
| 16b ² | 735 | 744 | −9 | 0.03 | 0.32 |
| 6a ² | 899 | 894 | +5 | 0.2 | 0.40 |
| 12 ¹ | 939 | 912 | +27 | 0.09 | 0.33 |
| 18a ¹ | 996 | 990 | +6 | 0.04 | 0.15 |
| 9a ¹ | 1116 | 1137 | −21 | 0.7 | 0.43 |
| 13 ¹ | 1147 | 1164 | −17 | 0.07 | 0.36 |
| 6a ¹ 16b ² | 1180 | 1191 | −11 | 0.02 | 0.33 |
| 6a ¹ $\gamma\text{CC}^1\gamma\text{CH}^1$ | 1267 | 1261 | +6 | 0.002 | 0.27 |
| 6a ³ | 1356 | 1342 | +14 | 0.05 | 0.19 |
| 6a ¹ 12 ¹ | 1389 | 1358 | +31 | 0.08 | 0.25 |
| 6a ¹ 18a ¹ | 1423 | 1437 | −14 | 0.02 | 0.25 |
| 19a ¹ | 1467 | 1478 | −11 | 0.3 | 0.33 |
| 8a ¹ | 1546 | 1552 | −6 | 0.09 | 0.38 |
| 6a ¹ 9a ¹ | 1570 | 1584 | −14 | 0.5 | 0.45 |
| 6a ¹ 13 ¹ | 1596 | 1611 | −15 | 0.04 | 0.30 |
| 6a ² 16b ² | 1626 | 1638 | −12 | 0.005 | 0.23 |
| 12 ¹ 16b ² | 1645 | 1656 | −11 | 0.003 | 0.22 |
| 17b ² | 1686 | 1684 | +2 | 0.0009 | 0.11 |
| 16b ² 18a ¹ | 1718 | 1735 | −17 | 0.0008 | 0.16 |
| 6a ⁴ | 1780 | 1788 | −8 | 0.007 | 0.05 |
| 6a ² 12 ¹ | 1840 | 1805 | +35 | 0.03 | 0.20 |
| 6a ¹ 19a ¹ | 1910 | 1925 | −15 | 0.2 | 0.28 |
| 6a ¹ 8a ¹ | 1998 | 1999 | −1 | 0.07 | 0.24 |
| 6a ² 9a ¹ | 2020 | 2031 | −11 | 0.1 | 0.18 |
| 9a ¹ 12 ¹ | 2053 | 2049 | +4 | 0.1 | 0.21 |
| 12 ¹ 13 ¹ | 2090 | 2075 | +15 | 0.007 | 0.12 |
| 9a ¹ 18a ¹ | 2132 | 2128 | +4 | 0.03 | 0.08 |

^a Wilson notation. ^b The symmetries of all the levels are a_1 , except for that of 6b¹ level. ^c A composite band of 6b¹ and 10b¹16b¹. ^d Intensities are normalized to the 0–0 band.

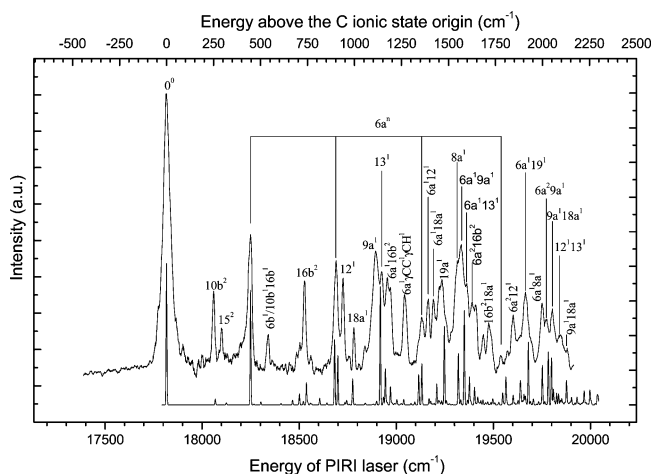


Figure 1. (Upper) parent PIRI spectrum of phenylacetylene cation in the \tilde{C}^2B_1 excited state, obtained via the origin of the ground ionic state. (Lower) simulated spectrum of the \tilde{C}^2B_1 state, where the square root of calculated intensity was used for comparison with the experimental one. The x-scale at the top of the figure corresponds to the vibrational energy of the \tilde{C}^2B_1 state.

Franck–Condon factors with the values of 0.09, 0.04, 0.07 and 0.09, respectively, compared to those three a_1 fundamentals mentioned above. However, 12¹, 18a¹ and 13¹ can be recognized in the spectrum at the positions near to their calculated frequencies, 912, 990, and 1164 cm^{-1} , respectively. A shoulder at 1546 cm^{-1} can be assigned as 8a¹, whose calculated frequency is 1552 cm^{-1} . The calculated frequencies of the remaining two

a_1 modes, 1 and ν_{CC} , are 728 and 2005 cm^{-1} , respectively. Although there are vibrational peaks in the spectrum near the calculated frequencies, we are reluctant to assign them as 1¹ and ν_{CC}^1 , because their calculated Franck–Condon factors are extremely small. Those peaks, however, will be assigned as overtones and combinations with overall a_1 symmetry, as will be discussed below.

For overtone and combination bands, the calculated Franck–Condon factors predict that $6a^n$ overtones and combinations of 6a and other a_1 modes should appear prominently. This has been observed in the PIRI study of the \tilde{B}^2B_1 states of other substituted benzene cations, fluorobenzene⁹ and chlorobenzene,¹⁰ as well as the MATI study of the ground state of phenylacetylene cation.¹⁹ Hence, the distinct peaks at 899, 1356 and 1780 cm^{-1} can be assigned as $6a^2$, $6a^3$, and $6a^4$ overtones, respectively. Also, the distinct peaks at 1389, 1423, 1570, 1840, 1910, 1998 and 2020 cm^{-1} can be assigned to combination bands, $6a^1 12^1$, $6a^1 18a^1$, $6a^1 9a^1$, $6a^2 12^1$, $6a^1 19a^1$, $6a^1 8a^1$ and $6a^2 9a^1$, respectively, and a shoulder at 1596 cm^{-1} is assigned as $6a^1 13^1$, on the basis of the calculated frequencies and Franck–Condon factors. Three peaks over 2050 cm^{-1} are assigned as combinations of other a_1 modes, $9a^1 12^1$, $12^1 13^1$, and $9a^1 18a^1$, with calculated frequencies of 2049, 2075, and 2128 cm^{-1} , respectively.

Most remaining distinct peaks can be assigned as overtones and combinations of nontotally symmetric modes with a_1 overall symmetry. Franck–Condon factor calculations show the $16b^2$ overtone and the $6a^1 16b^2$ combination, for which the calculated frequencies are 744 and 1191 cm^{-1} , should prominently appear in the spectrum because of the relatively significant Franck–Condon factors of 0.03 and 0.02. Thus, the vibrational peaks at 735 and 1180 cm^{-1} are assigned to those two transitions. Four peaks appearing in the spectrum at 1626, 1645, 1686 and 1718 cm^{-1} are assigned as $6a^2 16b^2$, $12^1 16b^2$, $17b^2$, and $16b^2 18a^1$. The actual intensities of these peaks are not as small, as expected from the Franck–Condon calculation. However, they might borrow the intensity from nearby strong transitions of a_1 vibrational modes through Fermi resonance coupling. Two peaks appearing in the spectrum at low energy around 250 cm^{-1} can only be assigned as $10b^2$ and 15^2 according to the calculated frequencies, even though the Franck–Condon factors are small.

The most challenging assignments are for the two distinct peaks at 539 and 1267 cm^{-1} , which do not show up in the simulations. Because the fundamental of the 6b mode, which has b_2 symmetry, appears in the MATI spectrum of the ground state of phenylacetylene cation¹⁹ and the PIRI spectra of the \tilde{B}^2B_1 states of fluorobenzene⁹ and chlorobenzene¹⁰ cations, we expect that it will also appear in the PIRI spectrum of the \tilde{C}^2B_1 state of phenylacetylene cation through vibronic coupling. The \tilde{A} ionic state has A_2 symmetry and small, but finite, oscillator strength from the \tilde{X} state (as determined by SAC–CI calculations), so vibronic coupling can occur between the \tilde{C} and \tilde{A} states, introducing intensity to a b_2 vibrational mode. The calculated frequency of $6b^1$ (612 cm^{-1}), however, is rather larger than 539 cm^{-1} , but vibronic coupling often causes calculated frequencies to be less accurate, and the intensity cannot be predicted by a calculated Franck–Condon factor. Thus the 539 cm^{-1} peak could be $6b^1$. However, calculations do indicate that another vibration, $10b^1 16b^1$, with a calculated frequency of 502 cm^{-1} and a nonzero Franck–Condon factor, could also be possibility. For the peak at 1267 cm^{-1} , the FC calculations suggest two transitions, $6b^2$ and $6a^1 \gamma_{CC}^1 \gamma_{CH}^1$, with the same factors of 0.002 and calculated frequencies of 1225 and 1262 cm^{-1} . However, if $6b^1$ is assigned to the 539 cm^{-1}

peak, which is reasonable as discussed above, $6b^2$ would be expected to appear at $\sim 1080 \text{ cm}^{-1}$ and will be buried in the strong $9a^1$ transition. Thus, we would prefer to assign the peak appearing at 1267 cm^{-1} in the PIRI spectrum as $6a^1 \gamma_{CC}^1 \gamma_{CH}^1$.

Conclusion

The vibrational structure of the \tilde{C} state of phenylacetylene cation is quite well resolved, although the line widths are not quite as narrow as some other substituted benzenes previously studied. The allowed transition from the ionic ground state is well determined by electronic structure calculations of the vibrational modes, and resulting Franck–Condon factors. Only two prominent lines are not adequately described by the calculations and could be indicative of vibronic coupling.

The symmetry of the \tilde{C} state is determined to be 2B_1 from the vibrational analysis, in agreement with electronic structure calculations and previous work.

Acknowledgment. Work at Stony Brook University was carried out under Contract No. DE-FG02-86ER13590 and at Brookhaven National Laboratory under Contract No. DE-AC02-98CH10886, both with the U.S. Department of Energy and supported by its Division of Chemical Sciences, Office of Basic Energy Sciences.

References and Notes

- (1) Johnson, P. M.; Anand, R.; Hofstein, J. D.; LeClaire, J. E. *J. Electron Spectrosc.* **2000**, *108*, 177.
- (2) Müller-Dethlefs, K.; Schlag, E. W. *Annu. Rev. Phys. Chem.* **1991**, *42*, 109.
- (3) Zhu, L. C.; Johnson, P. *J. Chem. Phys.* **1991**, *94*, 5769.
- (4) For a review, see: Eland, J. H. D. *Photoelectron Spectroscopy*, 2nd ed.; Butterworths: London, 1984. Kimura, K.; Katsumata, S.; Achiba, Y.; Yamazaki, T.; Iwata, S. *Handbook of He I Photoelectron Spectra of Fundamental Organic Molecules*; Japan Scientific Societies Press: Tokyo, 1981.
- (5) Taylor, D. P.; Goode, J. G.; LeClaire, J. E.; Johnson, P. M. *J. Chem. Phys.* **1995**, *103*, 6293.
- (6) Goode, J. G.; LeClaire, J. E.; Johnson, P. M. *Int. J. Mass Spectrom Ion Processes* **1996**, *159*, 49.
- (7) Goode, J. G.; Hofstein, J. D.; Johnson, P. M. *J. Chem. Phys.* **1997**, *107*, 1703.
- (8) LeClaire, J. E.; Anand, R.; Johnson, P. M. *J. Chem. Phys.* **1997**, *106*, 6785.
- (9) Anand, R.; LeClaire, J. E.; Johnson, P. M. *J. Phys. Chem. A* **1999**, *103*, 2618.
- (10) Anand, R.; Hofstein, J. D.; LeClaire, J. E.; Johnson, P. M.; Cossart-Magos, C. *J. Phys. Chem. A* **1999**, *103*, 8927.
- (11) Philis, J. G.; Drougas, E.; Kosmas, A. M. *Chem. Phys.* **2004**, *306*, 253.
- (12) Narayanan, K.; Chang, G. C.; Shieh, K. C.; Tung, C. C. *Spectrochim. Acta A* **1996**, *52*, 1703.
- (13) Ribblett, J. W.; Borst, D. R.; Pratt, D. W. *J. Chem. Phys.* **1999**, *111*, 8454.
- (14) Amatatsu, Y.; Hasebe, Y. *J. Phys. Chem. A* **2003**, *107*, 11169.
- (15) Serrano-Andres, L.; Merchán, M.; Jablonski, M. *J. Chem. Phys.* **2003**, *119*, 4294.
- (16) Rabalais, J. W.; Colton, R. J. *J. Electron Spectrosc.* **1973**, *1*, 83.
- (17) Lichtenberger, D. L.; Renshaw, S. K.; Bullock, R. M. *J. Am. Chem. Soc.* **1993**, *115*, 3276.
- (18) Dyke, J. M.; Ozeki, H.; Takahashi, M.; Cockett, M. C. R.; Kimura, K. *J. Chem. Phys.* **1992**, *97*, 8926.
- (19) Kwon, C. H.; Kim, H. L.; Kim, M. S. *J. Phys. Chem. A* **2003**, *107*, 10969.
- (20) Schmidt, M. W.; Baldrige, K. K.; Boatz, J. A.; Elbert, S. T.; Gordon, M. S.; Jensen, J. H.; Koseki, S.; Matsunaga, N.; Nguyen, K. A.; Su, S. J.; Windus, T. L.; Dupuis, M.; Montgomery, J. A. *J. Comput. Chem.* **1993**, *14*, 1347.
- (21) Borrelli, R.; Peluso, A. *J. Chem. Phys.* **2003**, *119*, 8437.
- (22) Wilson, E. B. *Phys. Rev.* **1934**, *45*, 0706.
- (23) Herzberg, D. *Molecular Spectra and Molecular Structure. II. Infrared and Raman Spectra of Polyatomic Molecules*; Van Nostrand: New York, 1945.